

# A Vector-Controlled PMSM Drive with a Continually On-Line Learning Hybrid Neural-Network Model-Following Speed Controller

Fayez F. M. El-Sousy<sup>†</sup>

Electronics Research Institute (ERI)  
Power Electronics & Energy Conversion Department, Cairo, Egypt

## ABSTRACT

A high-performance robust hybrid speed controller for a permanent-magnet synchronous motor (PMSM) drive with an on-line trained neural-network model-following controller (NNMFC) is proposed. The robust hybrid controller is a two-degrees-of-freedom (2DOF) integral plus proportional & rate feedback (I-PD) with neural-network model-following (NNMF) speed controller (2DOF I-PD NNMFC). The robust controller combines the merits of the 2DOF I-PD controller and the NNMF controller to regulate the speed of a PMSM drive. First, a systematic mathematical procedure is derived to calculate the parameters of the synchronous  $d-q$  axes PI current controllers and the 2DOF I-PD speed controller according to the required specifications for the PMSM drive system. Then, the resulting closed loop transfer function of the PMSM drive system including the current control loop is used as the reference model. In addition to the 2DOF I-PD controller, a neural-network model-following controller whose weights are trained on-line is designed to realize high dynamic performance in disturbance rejection and tracking characteristics. According to the model-following error between the outputs of the reference model and the PMSM drive system, the NNMFC generates an adaptive control signal which is added to the 2DOF I-PD speed controller output to attain robust model-following characteristics under different operating conditions regardless of parameter variations and load disturbances. A computer simulation is developed to demonstrate the effectiveness of the proposed 2DOF I-PD NNMF controller. The results confirm that the proposed 2DOF I-PD NNMF speed controller produces rapid, robust performance and accurate response to the reference model regardless of load disturbances or PMSM parameter variations.

**Keywords:** PMSM, Vector Control, 2DOF I-PD Controller, Neural Network (NN), Model Following Controller (MFC).

## 1. Introduction

In recent years, advancements in magnetic materials, semiconductor power devices and control theories have led

permanent-magnet synchronous motor (PMSM) drives to play a vitally important role in motion-control applications. PMSMs are widely used in high-performance applications such as industrial robots and machine tools because of their compact size, high-power density, high air-gap flux density, high-torque/inertia ratio, high torque capability, high efficiency and durability. When compared with an induction motor drive, the PMSM has many advantages. For instance,

Manuscript received August 9, 2004; revised Feb. 28, 2005.

<sup>†</sup>Corresponding Author: fayez@eri.sci.eg

Tel: +202-310554, Fax: +202-3351631, ERI

it has higher efficiency because there are no rotor losses; it also has lower no-load current below the rated speed. In addition, its decoupling control performance is less sensitive to parameter variations of the motor.

To achieve fast dynamic response and smooth starting, the field oriented control (FOC) technique is used in the design of the PMSM drive system. Like any other machine, the PMSM is inherently non-linear and possesses a multivariable coupled control system with high-order complex dynamics<sup>[1]-[4]</sup>. Utilizing the FOC technique simplifies the dynamic model of the PMSM and the control scheme. The electromagnetic torque is generated proportional to the product of the stator current and the PM rotor flux. The two components are orthogonal which results in high-performance similar to a separately excited DC motor.

Feed-back control is a common requirement for PMSM drive systems. The most widely used controller in industrial applications is the proportional plus integral plus derivative (PID) controller. Also, modified structures of the PID such as proportional plus integral & rate feed-back (PI-D) and integral plus proportional & rate feed-back (I-PD) controllers are developed. However, as these controllers have one degree-of-freedom, they may not be able to provide good command tracking and load regulation response simultaneously. The 2DOF configuration has the advantage that it allows the controller to process command tracking and disturbance regulation performance separately. The controller consists of two parts, the feed-back controller and the feed-forward controller. The feed-back controller ensures the closed loop stability and provides a good rejection of load disturbances while the feed-forward controller meets the desired command tracking specifications<sup>[5]-[7]</sup>. The 2DOF I-PD configuration is proposed in this paper. The proposed FOC PMSM drive system is shown in Fig. 1.

Recently, several control techniques have been developed for improving the performance of PMSM drives. Much research has been done to apply a neural network to the control of PMSM drive systems to deal with the nonlinearities and uncertainties of the dynamic model of a PMSM<sup>[8]-[9]</sup>. It is well known that neural networks need to be trained and that their training is time consuming. High convergence accuracy and a high

convergence rate are desirable for the training of the neural network. The most popular training algorithm for a multi-layer neural network is back propagation<sup>[10-12]</sup>.

The aim of this paper is to design  $d$ - $q$  axes current controllers and, as proposed, a robust hybrid speed controller. The proposed controller consists of a 2DOF I-PD controller and a neural-network model-following controller (NNMFC) for a PMSM drive system. In order to design these feed-back controllers to meet robust stability and disturbance rejection specifications, a quantitative analysis and design procedure is developed to find the parameters of the currents and speed controllers. First, the field oriented control transfer functions of the PMSM are derived from the dynamic model at the synchronously rotating rotor reference frame with nominal parameters. Next, on the basis of these transfer functions, the  $d$ - $q$  axes PI current controllers are designed to achieve the time domain specifications of the current control loops. After that, the 2DOF I-PD speed controller is designed to meet the specifications of the speed control loop. The closed loop transfer function of the whole drive system is chosen as the reference model. A proposed on-line trained NNMFC is designed and added to the 2DOF I-PD speed controller output to compensate for the error between the reference model and the PMSM drive system output due to parameter variations and load disturbances. When the error occurs, an adaptive control signal will be generated automatically from the NNMFC to maintain the desired model following performance for the PMSM drive system. To verify the design of the proposed controllers and PMSM drive system performance, the overall system is simulated. The dynamic performance of the PMSM drive system has been studied under load changes and parameter variations. The simulation results are given to demonstrate the effectiveness of the proposed controllers.

## 2. Mathematical Model of the PMSM

The mathematical modeling of the PMSM in the stationary and synchronously rotating rotor reference frames can be derived as follows<sup>[1]-[2]</sup>.

### 2.1 PMSM Model in $d^s$ - $q^s$ Stationary Frame

The stator voltage equations in the  $d^s$ - $q^s$  stationary

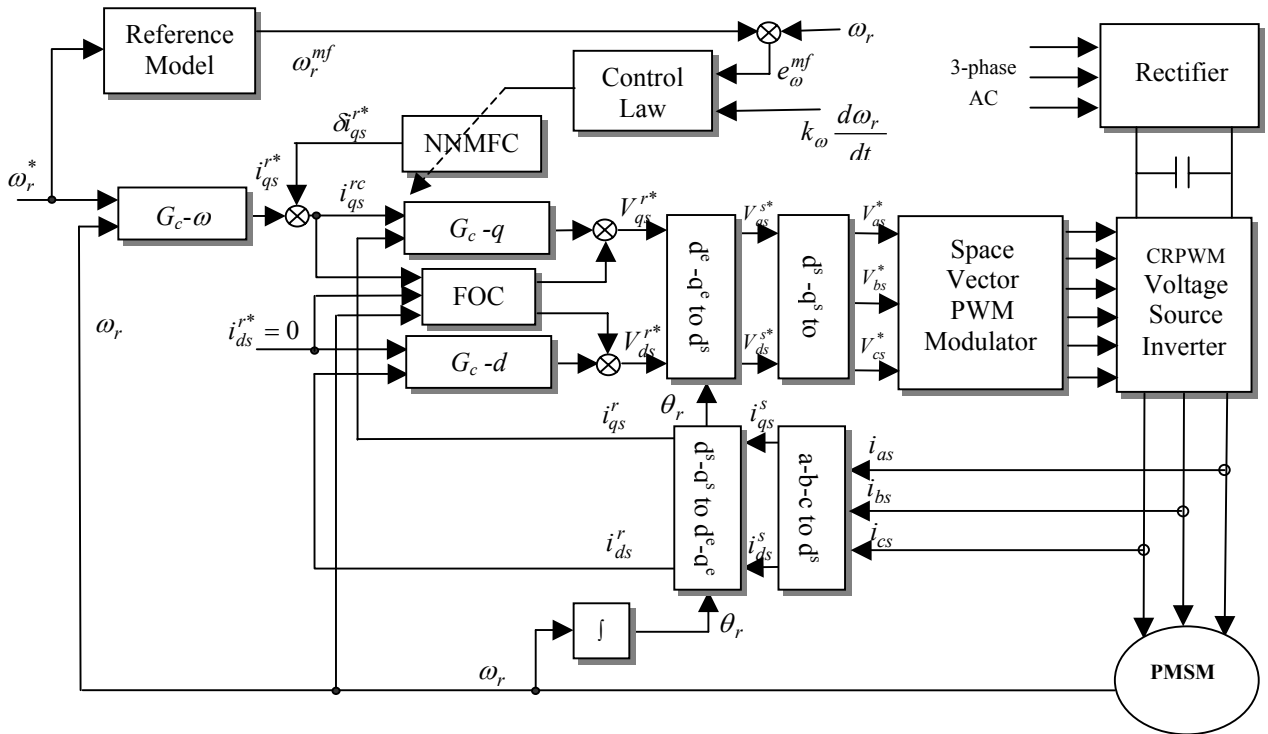


Fig. 1 The block schematic diagram of a field oriented PMSM drive system

frame can be expressed as follows:

$$\begin{aligned} V_{qs}^s &= R_s i_{qs}^s + L_{ss} \frac{di_{qs}^s}{dt} + \omega_r \lambda_m \cos(\theta_r) \\ V_{ds}^s &= R_s i_{ds}^s + L_{ss} \frac{di_{ds}^s}{dt} - \omega_r \lambda_m \sin(\theta_r) \end{aligned} \quad (1)$$

The electromagnetic torque can be expressed as:

$$T_e = \frac{3}{2} \cdot \frac{P}{2} \lambda_m [i_{qs}^s \cos(\theta_r) - i_{ds}^s \sin(\theta_r)] \quad (2)$$

The mechanical equation of the PMSM and load may be expressed as:

$$T_e = J_m \left( \frac{2}{P} \right) \frac{d}{dt} \omega_r + \beta_m \left( \frac{2}{P} \right) \omega_r + T_L \quad (3)$$

By choosing  $(i_{qs}^s, i_{ds}^s, \omega_r)$  as state variables, the PMSM state space representation in the stationary reference frame can be derived as follows:

$$\begin{aligned} \frac{d}{dt} \begin{bmatrix} i_{qs}^s \\ i_{ds}^s \end{bmatrix} &= \begin{bmatrix} -\frac{1}{\tau_s} & 0 \\ 0 & -\frac{1}{\tau_s} \end{bmatrix} \begin{bmatrix} i_{qs}^s \\ i_{ds}^s \end{bmatrix} + \frac{\lambda_m}{L_{ss}} \omega_r \begin{bmatrix} -\cos(\theta_r) \\ \sin(\theta_r) \end{bmatrix} \\ &+ \begin{bmatrix} -\frac{1}{L_{ss}} & 0 \\ 0 & +\frac{1}{L_{ss}} \end{bmatrix} \begin{bmatrix} V_{qs}^s \\ V_{ds}^s \end{bmatrix} \end{aligned} \quad (4)$$

$$\frac{d}{dt} \omega_r = T_e K_m - \frac{\beta_m}{J_m} \omega_r - K_m T_L \quad (5)$$

Where  $V_{qs}$ ,  $V_{ds}$ ,  $i_{qs}$  and  $i_{ds}$  are the stator voltages and currents respectively.  $R_s$ , and  $L_{ss}$  are the resistance and self inductance of the stator.  $\theta_r$ ,  $\omega_r$ ,  $J_m$ ,  $\beta_m$  and  $P$  are the rotor position, electrical rotor speed, effective inertia, friction coefficient and the number of poles of the motor respectively.  $T_e$ ,  $T_L$ , and  $\tau_s$  are the electromagnetic torque, the load torque and the stator time constant of the motor respectively.  $\lambda_m$ ,  $e_{qs}$  and  $e_{ds}$  are the flux linkage and the back emfs in the  $d$ - $q$  axes synchronous reference frame, respectively.

## 2.2 PMSM Model in the $d^r$ - $q^r$ Rotor Frame

The variables and parameters represented in the stationary reference frame can be transformed into the rotor reference frame as follows. The stator voltage equations in the  $d^r$ - $q^r$  synchronously rotating rotor reference frame and the electromagnetic torque can be carried out as follows:

$$V_{qs}^r = R_s i_{qs}^r + L_{ss} \frac{d}{dt} i_{qs}^r + \omega_r L_{ss} i_{ds}^r + \omega_r \lambda_m \quad (6)$$

$$V_{ds}^r = R_s i_{ds}^r + L_{ss} \frac{d}{dt} i_{ds}^r - \omega_r L_{ss} i_{qs}^r$$

$$T_e = \frac{3}{2} \cdot \frac{P}{2} \cdot \lambda_m i_{qs}^r \quad (7)$$

By selecting  $(i_{qs}^r, i_{ds}^r, \omega_r)$  as state variables, the state space equation of the PMSM can be given as follows:

$$\begin{bmatrix} \frac{d}{dt} i_{qs}^r \\ \frac{d}{dt} i_{ds}^r \end{bmatrix} = \begin{bmatrix} -\frac{1}{\tau_s} & \omega_r \\ \omega_r & -\frac{1}{\tau_s} \end{bmatrix} \begin{bmatrix} i_{qs}^r \\ i_{ds}^r \end{bmatrix} + \frac{\lambda_m}{L_{ss}} \begin{bmatrix} -\omega_r \\ 0 \end{bmatrix} \quad (8)$$

$$+ \begin{bmatrix} \frac{1}{L_{ss}} & 0 \\ 0 & \frac{1}{L_{ss}} \end{bmatrix} \begin{bmatrix} V_{qs}^r \\ V_{ds}^r \end{bmatrix}$$

$$\frac{d}{dt} \omega_r = K_t K_m \lambda_m i_{qs}^r - \frac{\beta_m}{J_m} \omega_r - K_m T_L \quad (9)$$

## 3. Field Oriented Control of the PMSM

In this paper, the field oriented control (FOC) technique is employed in order to obtain the high torque capability of the PMSM drive through decoupling the  $d$ - $q$  axes stator currents in the rotor reference frame. For a PMSM, the PM provides the flux linkage,  $\lambda_m$ . By keeping  $d$ -axis current,  $i_{ds}^r = 0$ , the PMSM torque may vary linearly with the  $q$ -axis current component,  $i_{qs}^r$ , and the maximum torque per ampere is achieved, which is similar to the control of a separately excited DC motor<sup>[4]</sup>.

## 4. Formulations and Configuration of the Proposed PMSM Drive System

The system configuration of the proposed speed control for a FOC PMSM drive system is illustrated in Fig. 2. It basically consists of a PI current controller in the  $q$ -axis and a 2DOF I-PD controller and a neural-network model-following controller. First, under nominal operating conditions, the PI current controller is designed based on the time domain specifications of the current loop. Then the 2DOF I-PD speed controller is designed based on the PMSM model to achieve the desired tracking and speed regulation performance. After that, a reference model is derived from the closed loop transfer function of the PMSM drive system shown in Fig. 2. Although the desired tracking and speed regulation can be obtained using the 2DOF I-PD speed controller with nominal PMSM parameters, the performance of the drive system is still sensitive to parameter variations. To solve this problem, a hybrid speed controller combining the 2DOF I-PD speed controller and the neural-network model-following controller (NNMFC) is proposed. The control law is designed as:

$$i_{qs}^{rc} = i_{qs}^{r*} + \delta i_{qs}^{r*} \quad (10)$$

$$e_{\omega}^{mf} = (\omega_r^{mf} - \omega_r) \quad (11)$$

$$\omega_r^* = k_{\omega} d\omega_r / dt$$

Where  $i_{qs}^{r*}$  is the  $q$ -axis current command generated from the 2DOF I-PD speed controller and  $\delta i_{qs}^{r*}$  is generated by the proposed NNMFC to automatically compensate for performance degradation. The inputs to the proposed NNMFC are the error signal  $e_{\omega}^{mf}$  and the derivative of the rotor speed that are used to train the weights of the neural-network controller on-line.  $\omega_r^{mf}$  is the output of the reference model while  $\omega_r$  is the rotor speed of the PMSM.

## 5. Designs of the Proposed Current and Speed Controllers

### 5.1 The *d*-*q* axes PI Current Controllers

This section considers the design of the current controller based on the voltage equation of the PMSM under FOC. The block diagram of the current control loop of the PMSM is shown in Fig. 3. The closed loop transfer function of the system is derived as follows.

$$\begin{aligned} \frac{i_{qds}^r(s)}{i_{qds}^{r*}(s)} &= \frac{(1/R_s\tau_s).(K_p^c s + K_i^c)}{s^2 + s(1/\tau_s + K_p^c/R_s\tau_s) + K_i^c/R_s\tau_s} \\ &\triangleq \frac{\omega_n^2}{s^2 + 2\zeta\omega_n s + \omega_n^2} \end{aligned} \quad (12)$$

From this equation the parameters of the PI controller can be found.

$$\begin{aligned} K_p^c &= \left( \frac{2\zeta\omega_n - 1/\tau_s}{R_s\tau_s} \right) \\ K_i^c &= \omega_n^2 R_s \tau_s \end{aligned} \quad (13)$$

### 5.2 The Proposed 2DOF I-PD Speed Controller

The controller consists of an I-PD feed-back controller and feed-forward controller as shown in Fig. 4. The I-PD feed-back controller is designed for load regulation and disturbance rejection, while the feed-forward controller is designed to attain the desired tracking speed response. To accomplish this objective, the denominator of the feed-forward controller is selected to cancel the numerator of the closed loop transfer function of the drive system<sup>[5]</sup>.

#### 5.2.1 The Feed-back I-PD Speed Controller

The closed loop transfer function of the PMSM drive system consisting only of the feed-back speed control with no load is derived according to Fig. 4. The controller parameters' relationships are derived from equation (14) as follows:

$$\begin{aligned} \frac{\omega_r(s)}{\omega_r^{d*}(s)} &= \frac{a_0(1+K_{PI}^c s)}{a_4 s^4 + a_3 s^3 + a_2 s^2 + a_1 s + a_0} \\ &\triangleq \frac{\omega_n^4}{s^4 + 2.1\omega_n s^3 + 3.4\omega_n^2 s^2 + 2.7\omega_n^3 s + \omega_n^4} \end{aligned} \quad (14)$$

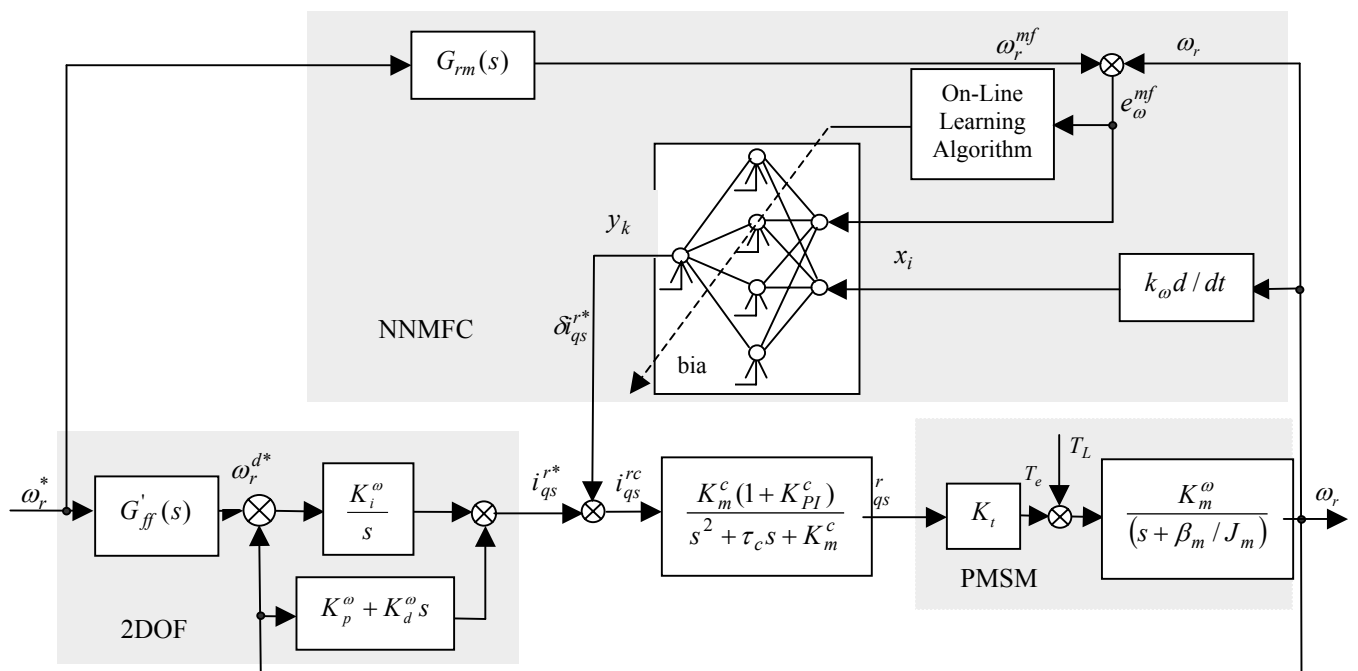


Fig. 2 Configuration of the proposed NNMFC speed controller for a field oriented PMSM drive system

$$K_p^\omega = \frac{\left(2.7\omega_n^3 - K_m^c \beta_m / J_m\right)}{K_m^\omega K_m^c K_t} \quad (15)$$

$$K_i^\omega = \frac{\omega_n^4}{K_m^\omega K_m^c K_t} \quad (16)$$

$$K_d^\omega = \frac{\left(3.4\omega_n^2 - K_m^c - \tau_c \beta_m / J_m\right)}{K_m^\omega K_m^c K_t} \quad (17)$$

### 5.2.2 The Feed-forward Speed Controller

The closed loop transfer function of the PMSM drive system including the feed-forward speed controller with no load is derived according to Fig. 4 as follows.

$$\begin{aligned} \frac{\omega_r(s)}{\omega_r^*(s)} &= \frac{a_o(1+K_{PI}^c s)}{a_4 s^4 + a_3 s^3 + a_2 s^2 + a_1 s + a_o} \cdot G_{ff}(s) \\ &\equiv \frac{\omega_n^4}{s^4 + 2.1\omega_n s^3 + 3.4\omega_n^2 s^2 + 2.7\omega_n^3 s + \omega_n^4} \end{aligned} \quad (18)$$

From equation (18), the feed-forward controller transfer function is given by:

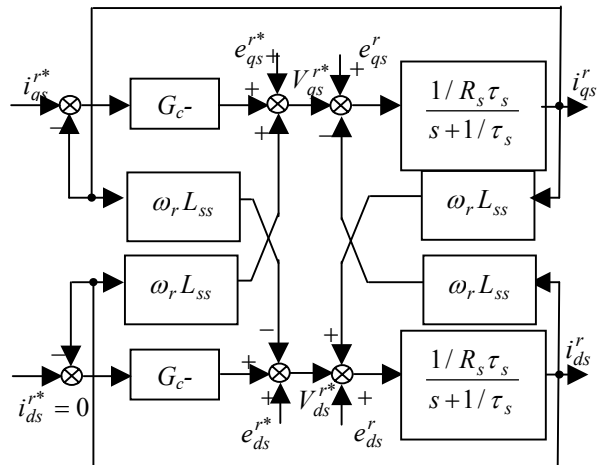


Fig. 3 Configuration of the synchronous PI current controllers

$$G_{ff}(s) = \frac{\omega_n^4}{K_m^\omega K_m^c K_t K_i^\omega (1+K_{PI}^c s)} \quad (19)$$

The above controller is a lag compensator but to improve the relative stability of the speed response, we

suggest a lead compensator which is added to the feed-forward controller transfer function as follows.

$$G'_{ff}(s) = \bar{K} \cdot \frac{(1+\tau_1 s)}{(1+\tau_2 s)} \quad (20)$$

The transfer function of the reference model with the 2DOF I-PD speed controller is derived according to the block diagram shown in Fig. 4 as follows.

$$G_{rm}(s) = \frac{\omega_r(s)}{\omega_r^*(s)} = \frac{b_o \bar{K} (1+\tau_1 s)}{b_3 s^3 + b_2 s^2 + b_1 s + b_o} \quad (21)$$

## 6. The Proposed Neural-Network Model - Following Speed Controller (NNMFC)

In this section, a proposed neural-network model-following controller (NNMFC) with on-line learning is introduced. The on-line trained NNMFC for the PMSM drive system is shown in Fig. 5. The inputs to the NNMFC are the error  $e_\omega^{mf}$  and  $k_\omega(d/dt)\omega_r$  while the output is the observed compensation signal  $\delta t_{qs}^{r*}$ . The error difference between the reference model and the output speed of the PMSM is used to train the weights and biases of the neural-controller to provide a good model-following response. The weights and biases are adjusted on-line to produce the required compensation signal. Utilizing this adaptive control signal will allow the drive system to follow the reference model.

### 6.1 Neural-Network for PMSM Drive System

The NNMFC comprises a three layer neural-network as shown in Fig. 5. The signal propagation and activation functions are introduced as follows.

#### 6.1.1 Input Layer

For every node  $i$  in the input layer, the neural-network input and output are expressed as:

$$nn_i = x_i \quad (22)$$

$$y_i = f_i(nn_i) \quad i = 1, 2 \quad (23)$$

$$x_1 = e_\omega^{mf}(t), \quad x_2 = k_\omega \frac{d}{dt}\omega_r \quad (24)$$

### 6.1.2 Hidden Layer

The input and output of the hidden layer to a node  $j$  are introduced, respectively, as follows.

$$nn_j = \sum_i (W_{ji}y_i) + \phi_j \quad (25)$$

$$y_j = f_j(nn_j) \quad j = 1, \dots, m \quad (26)$$

$$f_j(nn_j) = \frac{1}{1 + e^{-nn_j}} \quad (27)$$

### 6.1.3 Output Layer

The input of the output layer to a node  $k$  is given by:

$$nn_k = \sum_j (W_{kj}y_j) + \phi_k \quad (28)$$

And the corresponding output is

$$y_k = f_k(nn_k) = \frac{1}{1 + e^{-nn_k}} \quad (29)$$

$$y_k = \delta i_{qs}^{r*} \quad (30)$$

## 6.2 On-Line Training Algorithm

The back propagation training algorithm is an iterative gradient algorithm designed to minimize the mean square error between the actual output of a feed-forward net and the desired output. This technique uses a recursive algorithm starting at the output units and working back to the hidden layer to adjust the neural weights according to the following equations. The desired speed  $\omega_r^{mf}$  is obtained from the reference model as given by equation (21), thus the energy error function is defined as follows:

$$E_\omega = \frac{1}{2} \sum_N [\omega_r^{mf}(N) - \omega_r(N)]^2 = \frac{1}{2} \sum_N e_\omega^2(N) \quad (31)$$

Where  $\omega_r^{mf}(N)$  and  $\omega_r(N)$  are the outputs of the reference model and PMSM drive system at the  $N^{\text{th}}$ -iteration. Within each interval from  $N-1$  to  $N$ , the back propagation algorithm [13]-[15] is used to update the weights of the hidden and output layers in the NNMFC according to the following equations:

$$W_{ji}(N+1) = W_{ji}(N) - \varepsilon \frac{\partial E_\omega}{\partial W_{ji}(N)} + \gamma \Delta W_{ji}(N-1) \quad (32)$$

$$W_{kj}(N+1) = W_{kj}(N) - \varepsilon \frac{\partial E_\omega}{\partial W_{kj}(N)} + \gamma \Delta W_{kj}(N-1) \quad (33)$$

$$\Delta W_{ji}(N-1) = W_{ji}(N) - W_{ji}(N-1) \quad (34)$$

$$\Delta W_{kj}(N-1) = W_{kj}(N) - W_{kj}(N-1) \quad (35)$$

The required gradient of  $E_\omega$  in equation (31) between the output and hidden layers is determined according to the following equation.

$$\frac{\partial E_\omega}{\partial W_{kj}} = \frac{\partial E_\omega}{\partial nn_k} \cdot \frac{\partial nn_k}{\partial W_{kj}} = \frac{\partial E_\omega}{\partial nn_k} \cdot y_j \quad (36)$$

The error term to be propagated is given by:

$$\delta_k = \frac{\partial E_\omega}{\partial nn_k} = \sum \frac{\partial E_\omega}{\partial \omega_r} \cdot \frac{\partial \omega_r}{\partial i_{qs}^{c*}} \cdot \frac{\partial i_{qs}^{c*}}{\partial y_k} \cdot \frac{\partial y_k}{\partial nn_k} \quad (37)$$

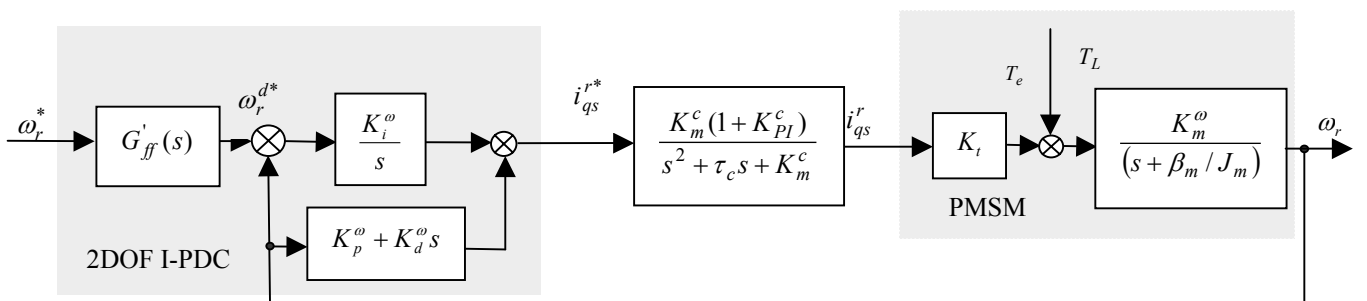


Fig. 4 Configuration of the speed control for PMSM using 2DOF I-PD speed controller

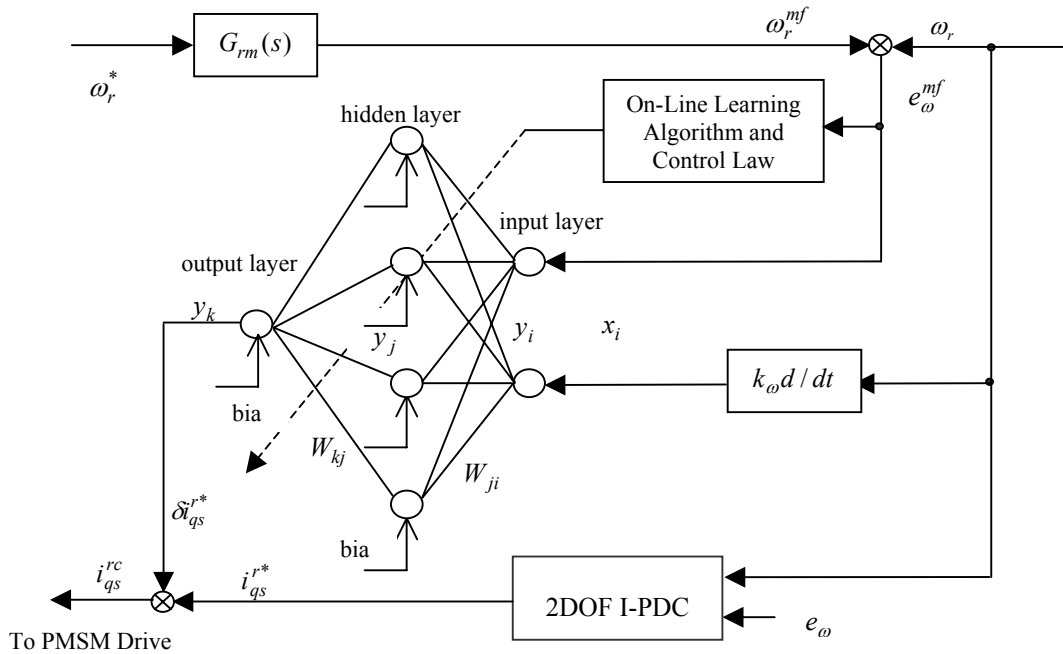


Fig. 5 The proposed neural-network model-following controller

The gradient of  $E_\omega$  between the hidden and input layers is determined according to the following equation.

$$\frac{\partial E_\omega}{\partial W_{ji}} = \frac{\partial E_\omega}{\partial nn_j} \cdot \frac{\partial nn_j}{\partial W_{ji}} = \frac{\partial E_\omega}{\partial nn_j} \cdot y_i \quad (38)$$

The error term to be propagated is given by:

$$\delta_j = \frac{\partial E_\omega}{\partial nn_j} = \sum \frac{\partial E_\omega}{\partial nn_k} \cdot \frac{\partial nn_k}{\partial y_j} \cdot \frac{\partial y_j}{\partial nn_j} \quad (39)$$

$$\delta_j = \sum \delta_k W_{kj} f'(nn_j) \quad (40)$$

To increase the on-line learning rate of the weights, a control law is proposed as follows.

$$\frac{\partial E_\omega}{\partial y_k} = e_\omega^{mf} - k_\omega (d/dt) \omega_r \quad (41)$$

Where,  $x_i$  is the inputs to the nodes of the input layer;  $y_{i,j,k}$  is the outputs from the nodes of the input, hidden and output layers;  $f_{i,j,k}$  are the sigmoid functions of input,

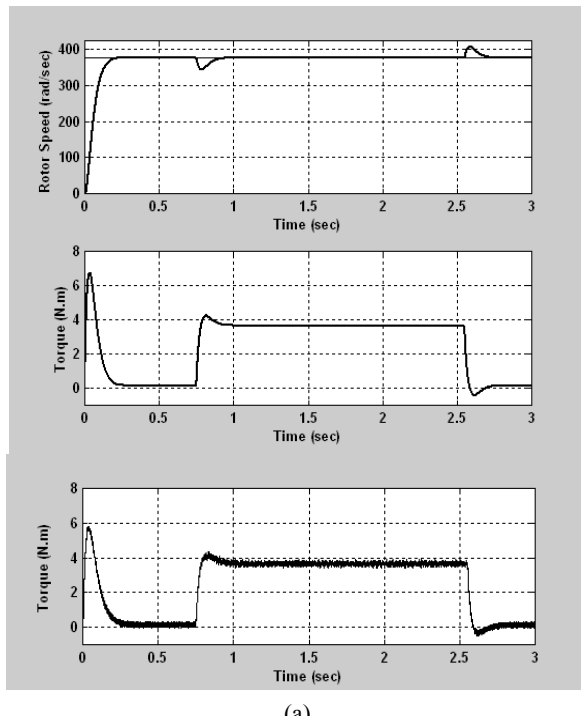
hidden and output layers;  $W_{ji}$  is the weight between the input and hidden layers;  $W_{kj}$  is the weight between the hidden and output layers;  $\phi_{kj}$  is the bias between the hidden and output layers;  $\gamma$  is the momentum factor; and  $\varepsilon$  is the learning rate.

## 7. Simulation Results of the PMSM Drive

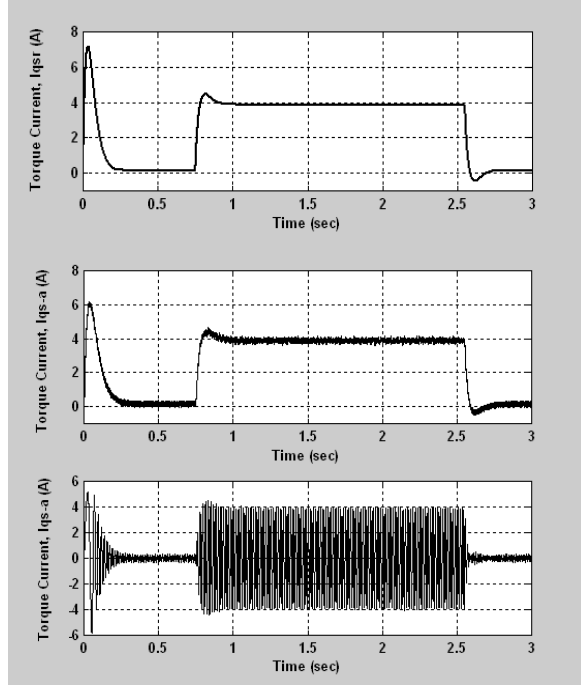
The efficacy of the proposed scheme for the PMSM drive system shown in Fig. 1 is verified by computer simulations based on MATLAB/SIMULINK<sup>[4],[16]-[17]</sup>. The parameters of the PMSM are given in Table 1. As mentioned before, this paper proposes a robust hybrid 2DOF I-PD NNMFC speed controller.

### 7.1 Dynamic Performance at NP

The simulation results of the PMSM drive system with nominal parameters (NP) are presented to verify the feasibility of the proposed control scheme under various operating conditions. The dynamic performance of the drive system with a step speed command of 377 rad/sec under no-load and with a load of 3.6 N.m is predicted as illustrated in Figs. 6-7. The disturbance rejection

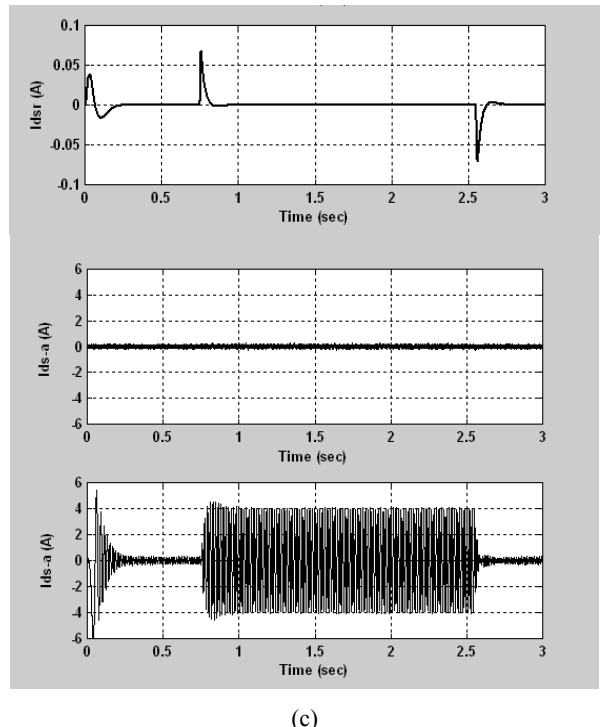


(a)



(b)

capabilities have been checked when a load of 3.6 N.m is applied to the shaft at  $t = 0.75$ s and removed after a period of 1.8s. The simulation results of the proposed 2DOF I-PD speed controller are shown in Fig. 6. They include the

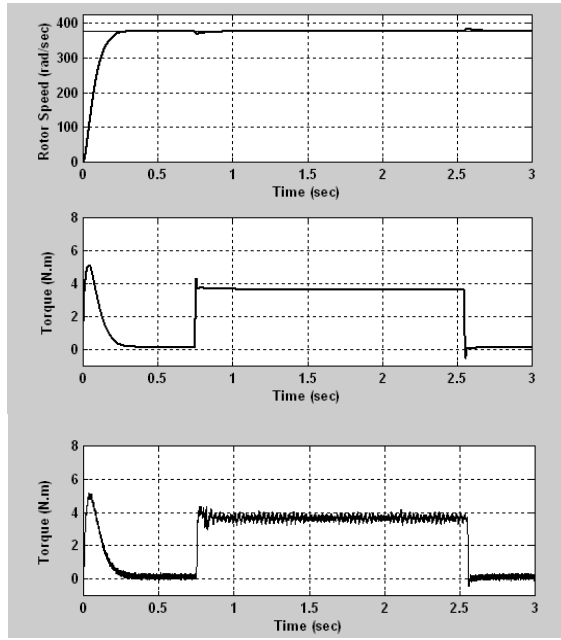


(c)

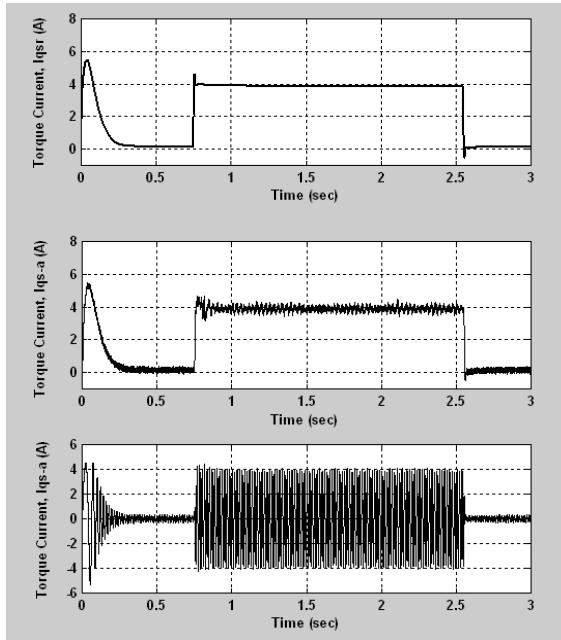
Fig. 6 Step speed response of a PMSM drive system using a 2DOF I-PD speed controller  
 (a) Speed and torque responses.  
 (b) Reference and actual  $q$ -axis stator current responses  
 (c) Reference and actual  $d$ -axis stator current responses

command and actual responses for speed, load regulation, torque, and  $d$ - $q$  axes stator currents. The dynamic performance utilizing the proposed hybrid 2DOF I-PD NNMFC speed controller is represented in Fig. 7. These figures clearly illustrate good dynamic performance in both command tracking and load regulation for each of the two controllers.

By using the proposed 2DOF I-PD NNMFC speed controller, improvements in control performance in both command tracking and load regulation can be observed in Fig. 8. It is clear from this figure that the proposed 2DOF I-PD NNMFC speed controller provides a rapid and accurate response to the reference model within 0.3 s. Also, the proposed controller quickly returns the speed to the reference value under a full load with a maximum dip of 8 rad/sec, compared to the 2DOF I-PD speed controller which shows a slow response to the reference model and a large dip in speed of about 35 rad/sec. The model-

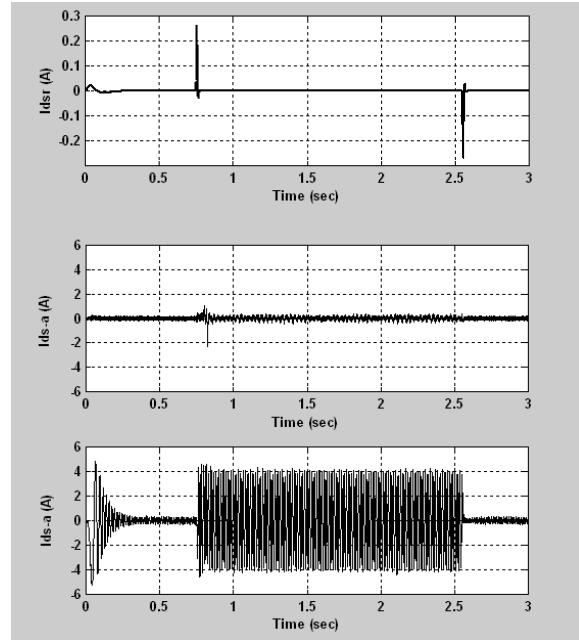


(a)



(b)

following response and the model-following error (MFE) for the PMSM drive system is shown for both speed controllers in Fig. 9. This figure shows that the model-following error (MFE) for the PMSM with 2DOF I-PD speed controller reaches 60 rad/sec, while the MFE for the PMSM with 2DOF I-PD NNMFC speed controller only reaches about 5 rad/sec. Therefore, the proposed



(c)

Fig. 7 Step speed response of a PMSM drive system using a 2DOF I-PD NNMFC speed controller

(a) Speed and torque responses.

(b) Reference and actual q-axis stator current responses

(c) Reference and actual d-axis stator current responses

model-following neural network controller provides a good model-following response.

## 7.2 Consideration of Parameter Variations

A simulation of the proposed 2DOF I-PD NNMFC approach demonstrates robust response to large variations in PMSM parameters and external load disturbances. The simulation results of the dynamic response for both currents and speed controllers are plotted in Figs. 10-12. To investigate the effectiveness of the proposed hybrid speed controller, three cases of parameter variations in motor inertia and load torque disturbance are considered. The following possible ranges of parameter variations and external disturbances are considered.

*Case 1:*  $J_m = J_m^*$ ,  $T_L = 0-3.5 \text{ N.m}$ .

*Case 2:*  $J_m = 0.25 \times J_m^*$ ,  $T_L = 0-3.5 \text{ N.m}$ .

*Case 3:*  $J_m = 5 \times J_m^*$ ,  $T_L = 0-3.5 \text{ N.m}$ .

The speed response and the load regulation

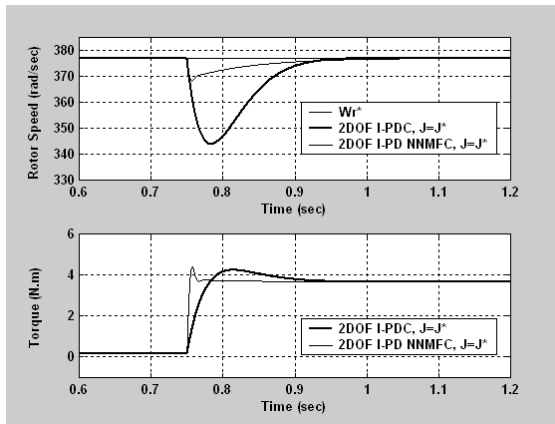


Fig. 8 The load regulation performance for both speed controllers with nominal parameters

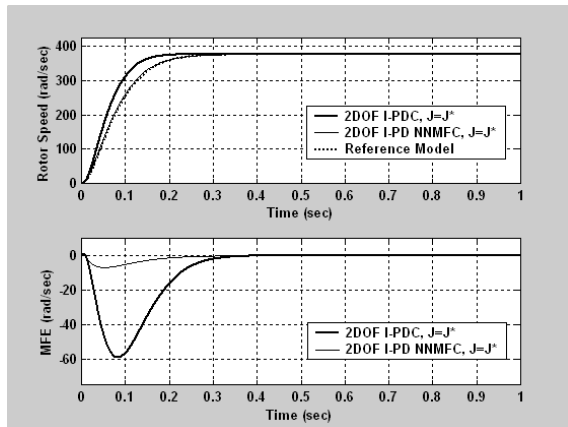
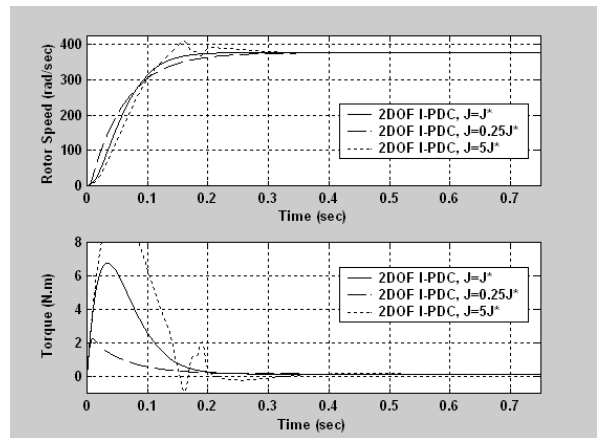
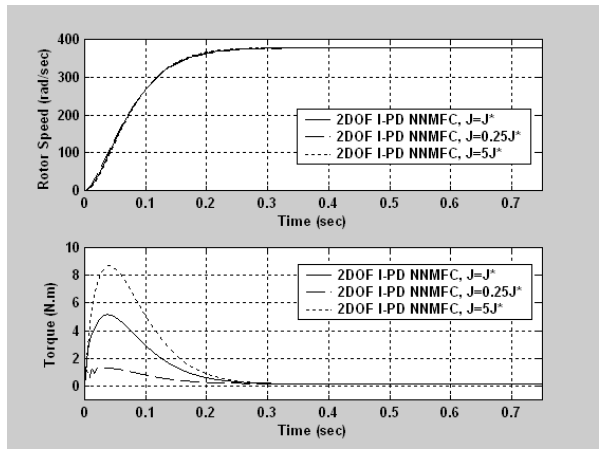


Fig. 9 The speed tracking response and (MFE) for both speed controllers under nominal parameters

performance of the drive system with the 2DOF I-PD and 2DOF I-PD NNMFC speed controllers are shown in Figs. 10-11 for the three cases of PMSM parameter variations. Fig. 10 illustrates the speed tracking and torque responses for both speed controllers. Under the same conditions, the load regulation performance and torque response are given in Fig. 11. The results shown in Figs. 10-11 clearly indicate that as the variations of the PMSM parameters occurred, the response of the 2DOF I-PD speed controller deviated significantly from the nominal case. On the other hand, the 2DOF I-PD NNMFC speed controller was only slightly influenced by the parameter variations and maintained correct operation. The results confirm the robust performance of the 2DOF I-PD NNMFC speed controller. The model-following error for both controllers



(a)



(b)

Fig. 10 Model following response of the PMSM drive system under parameter variations

(a) The 2DOF I-PD speed controller

(b) The 2DOF I-PD NNMFC speed controller

when exposed to parameter variations is shown in Fig. 12. We can observe from this figure that the 2DOF I-PD speed controller had a large MFE while the 2DOF I-PD NNMFC speed controller was insignificantly affected by parameter variations and had a very small MFE. From the above simulation results, it is evident that the 2DOF I-PD NNMFC speed controller performs satisfactorily as the PMSM drive system controller, even under load disturbances and parameter variations. Our results show good model-following tracking responses in all cases. Moreover, the regulation performance is much better, in both speed dip and recovery time, than that obtained by the 2DOF I-PD speed controller.

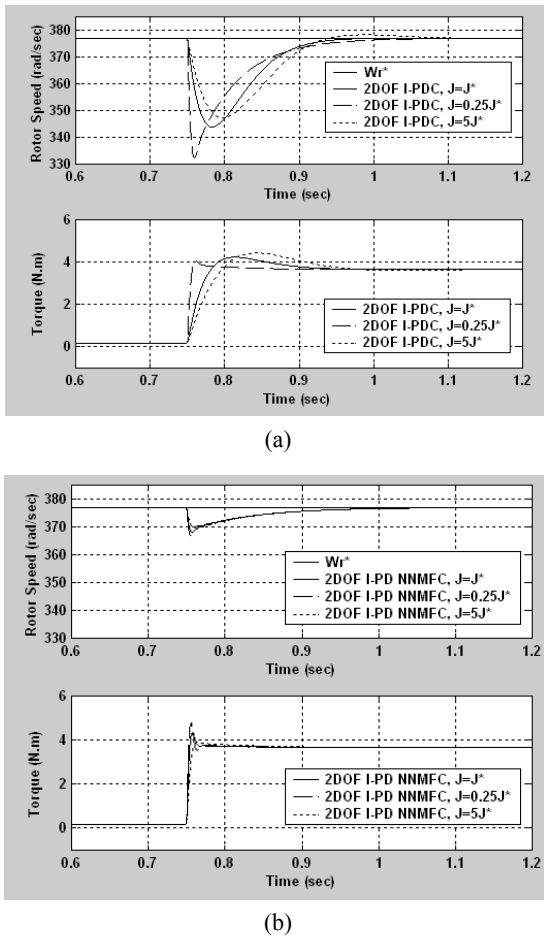


Fig. 11 The load regulation performance of the drive system under parameter variations  
 (a) The 2DOF I-PD speed controller  
 (b) The 2DOF I-PD NNMFC speed controller

## 8. Conclusions

This paper proposes a robust hybrid 2DOF I-PD NNMFC speed controller for PMSM drive systems under FOC which guarantees robustness in the presence of parameter variations. Quantitative design procedures for the 2DOF I-PD and 2DOF I-PD NNMFC controllers have been successfully developed. First, the I-PD speed controller was designed according to the given command tracking specifications and the closed loop transfer function was chosen as the reference model. Then, the feed-forward controller was designed as a lead/lag compensator to improve the disturbance rejection characteristics of the drive system. The performance of the drive system is still sensitive to parameter variations using the 2DOF I-PD

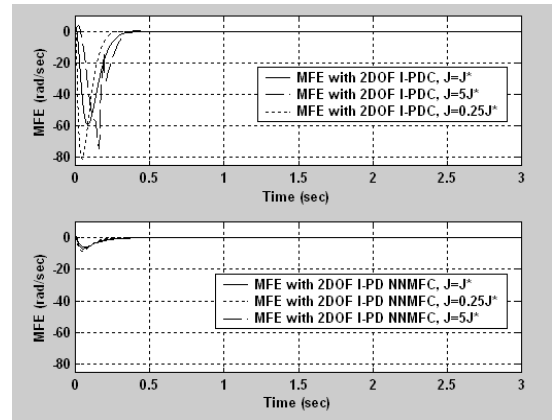


Fig. 12 The model-following error (MFE) for both speed controllers under parameter variations

speed controller. To solve this problem, a NNMFC with on-line learning was designed and added to the 2DOF I-PD speed controller to preserve the good model-following characteristics in the face of parameter variations and external disturbances. The NNMFC provides an adaptive feed-back control signal based on the error between the reference model and the output speed of PMSM in order to allow the drive system to follow the reference model. This error was used to train the weights and biases of the NNMFC to provide a good model-following response. As a result, the rotor speed tracking response can be controlled to closely follow the response of the reference model under a wide range of operating conditions. The performance of the drive system and the effectiveness of the proposed controllers have been demonstrated by a wide range of simulation results. Simulation results have shown that the proposed 2DOF I-PD NNMFC speed controller grants accurate tracking and regulation characteristics in the face of PMSM parameter variations and external load disturbance. Also, a robust model-following tracking response is obtained utilizing the I-PD NNMFC speed controller.

## Appendix

Table 1 PMSM parameters

Type: three-phase PMSM, 1 hp, 4 poles, 208 V, 60 Hz, 1800 rpm, Voltage constant: 0.314 V.s/rad, Torque constant: 0.95 N.m/A,  $R_s=1.5 \Omega$ ,  $L_{ss}=L_d=L_q=0.05 \text{ H}$ ,  $J_m=0.003 \text{ kg.m}^2$ ,  $\beta_m=0.0009 \text{ N.m/rad/sec}$

$$\begin{aligned}
K_m^\omega &= (P/2)/J_m, \quad K_t = (3P/4)\lambda_m, \quad K_{PI}^c = K_p^c/K_i^c, \\
\tau_s &= L_s/R_s, \quad K_m^c = K_i^c/R_s\tau_s, \quad \tau_c = (1/\tau_s + K_p^c/R_s\tau_s), \\
\bar{K} &= \omega_n^4 / K_m^\omega K_m^c K_t K_i^\omega, \quad \theta_r(t) = \int \omega_r(t) dt, \\
a_o &= K_i^\omega K_m^\omega K_m^c K_t, \\
a_1 &= (K_m^c \beta_m / J_m + K_m^\omega K_m^c K_t K_p^\omega + a_o K_{PI}^c), \\
a_2 &= (K_m^c + \tau_c \beta_m / J_m + K_m^\omega K_m^c K_t K_d^\omega + K_m^\omega K_m^c K_t K_p^\omega K_{PI}^c), \\
a_3 &= (\tau_c + \beta_m / J_m + K_m^\omega K_m^c K_t K_d^\omega K_{PI}^c), \quad a_4 = 1, \\
b_o &= K_i^\omega K_m^\omega K_t, \quad b_1 = (\beta_m / J_m + K_m^\omega K_t K_p^\omega + b_o \tau_2), \\
b_2 &= (1 + \tau_2 \beta_m / J_m + K_m^\omega K_t K_d^\omega + K_m^\omega K_t K_p^\omega \tau_2), \\
b_3 &= (\tau_2 + K_m^\omega K_t K_d^\omega \tau_2)
\end{aligned}$$

## References

- [1] P.C. Krause, Analysis of Electric Machinery, New York, McGraw Hill, 1986.
- [2] B. K. Bose, Modern Power Electronics and AC Drives, Prentice Hall, Upper Saddle River, 2002.
- [3] Peter Vas, Vector Control of AC Machines, Oxford: Clarendon Press, 1990.
- [4] Ned Mohan, Advanced Electric Drives: Analysis, control, and Modeling using Simulink, MNPERE Press, USA, 2001.
- [5] Fayed F. M. El-Sousy, "Design and Implementation of 2DOF I-PD Controller for Indirect Field Orientation Control Induction Machine Drive System", ISIE 2001 IEEE International Symposium on Industrial Electronics, Pusan, Korea, June 12-16, pp. 1112-1118, 2001.
- [6] C. M. Liaw, "Design of a two-degrees-of-freedom controller for motor drives", IEEE Trans. Automatic Control, Vol. AC-37, No. 4, Aug./Sept., pp. 1215-1220, 1992.
- [7] Fayed F. M. El-Sousy and Maged N. F. Nashed, "Robust Fuzzy Logic Current and Speed Controllers for Field-Oriented Induction Motor Drive", The Korean Institute of Power Electronics (KIPE), Journal of Power Electronics (JPE), Vol. 3, No. 2, pp. 115-123, April 2003.
- [8] M. A El-Sharkawy, "Neural network application to high performance electric drive system", Proceeding of ICEON'95, pp. 44-496, 1995.
- [9] Fayed F. M. El-Sousy and M. M. Salem, "Simple Neuro-Controllers for Field Oriented Induction Motor Servo Drive System", The Korean Institute of Power Electronics (KIPE), Journal of Power Electronics (JPE), Vol. 4, No. 1, pp. 28-38, January 2004.
- [10] K. S. Narendra and K. Parthasarathy, "Identification and control of dynamical systems using neural networks", IEEE Trans., Neural Network, NN-1, pp. 4-27, 1990.
- [11] T. Fukuda and T. Shibata, "Theory and applications of neural networks for industrial control systems", IEEE Trans., Ind. Electr., IE-39, pp. 472-491, 1992.
- [12] Yang Yi, D. Mahinda Vilathgamuwa and Azizur Rahman, "Implementation of an Artificial-Neural-Network-Based Real-Time Adaptive Controller for an Interior Permanent-Magnet Motor Drive", IEEE Trans., Ind. Applic., IA-39, No. 1, pp. 96-104, 2003.
- [13] Faa-Jeng and Chih-Hong Lin, "A Permanent-Magnet Synchronous Motor Servo Drive Using Self-Constructing Fuzzy Neural Network Controller", IEEE Trans., Energy Conversion, EC-19, No. 1, pp. 66-72, 2004.
- [14] Fayed F. M. El-Sousy and M. M. Salem, "High Performance Simple Position Neuro-Controller for Field-Oriented Induction Motor Servo Drives", WSEAS Transactions on Systems, Issue 2, Vol. 3, pp. 941-950, April 2004.
- [15] Fayed F. M. El-Sousy, "A High-Performance Induction Motor Drive with 2DOF I-PD Model-Following Speed Controller", The Korean Institute of Power Electronics (KIPE), Journal of Power Electronics (JPE), Vol. 4, No. 4, pp. 217-227, October 2004.
- [16] Matlab Simulink User Guide, The Math Work Inc., 1997
- [17] C. M. Ong, Dynamic Simulation of Electric Machinery Using Matlab and Simulink, Printice Hall, 1998.



**Fayed Fahim El-Sousy** was born in Gahrbia Prefecture, Egypt in 1965. He received the B.Sc. degree in Electrical Power and Machines Engineering from Menoufia University, Egypt in 1988, the M.Sc. degree in Electrical Power and Machines Engineering from Cairo University, Egypt in 1994 and the Ph.D degree in Electrical Power and Machines Engineering from Cairo University, Egypt in 2000. Since 1990, he has been with the Department of Power Electronics and Energy Conversion at the Electronics Research Institute (ERI) where he is currently an Assistant Professor. From April 2004 to October 2004 he was a Post Doctoral visiting researcher at Kyushu University, Graduate School of Information Science and Electrical Engineering, Energy Conversion Laboratory, Japan. His research interests are in the areas of modeling and control of IM, PMSM, LIM and PMLSM drives, intelligent control, optimal control and power electronics. Dr. El-Sousy is currently interested in the robust control of the linear motor Maglev drive system.